Journal of Agrosystems and Analytics
Volume 1 Issue 1 2026 (Jan-June 2026) | Page No:- 15-24

RESEARCH ARTICLE

Assessment of Future Climate Change Projections in South Gujarat Using Bias-Corrected GCMs

V. B. Virani[1*], Dr. M. H. Amlani[2], B. M. Mote[1]

[1]Agricultural Meteorological Cell, Navsari Agricultural University, Navsari, Gujarat, India

[2]College of Forestry, Navsari Agricultural University, Navsari, Gujarat, India

(*Received 6 January 2026, Accepted 15 March 2026*)

***Corresponding author:** vivekvirani9999@gmail.com

Abstract

The study aims to assess the climate change projections in South Gujarat region using bias-corrected General Circulation Model (GCM) projections under SSP245 and SSP585 scenarios. For maximum temperature, the chosen models were ACCESS-CM2, CMCC-ESM2, GFDL-CM4, KIOST-ESM, and TaiESM1. For minimum temperature, ACCESS-ESM1-5, CNRM-ESM2-1, EC-Earth3, and INM-CM5-0 were selected. The models identified for rainfall simulation included ACCESS-CM2, KACE-1-0-G, MPI-ESM1-2-LR, MRI-ESM2-0, and TaiESM1. These models were selected based on their accuracy in representing historical climate data and their applicability for future climate projections in the study region. Under SSP585, maximum temperature is projected to rise by 2.4 °C and minimum temperature by over 5.6 °C by the end of the century. Rainfall projections suggest a potential increase of up to 14.50% by 2090. An evaluation of GCM bias correction methods revealed that Quantile Mapping (QM) significantly outperformed Linear Scaling (LS) in reducing Root Mean Square Error (RMSE). While LS struggled with complex deviations, QM effectively corrected distributional biases and extreme outliers across temperature and precipitation datasets, proving essential for reliable climate modeling.

Keywords: GCMs; Climate change; Gujarat; CMIP6; Bias correction; SSPs

1. Introduction

Climate change is the long-term shift in temperature, precipitation, wind patterns, and other climatic factors of the Earth, influenced by both natural processes and human-induced activities, particularly greenhouse gas emissions (IPCC, 2021). Over the last hundred years, human activities, including the burning of fossil fuels, deforestation, and industrial expansion, have substantially raised atmospheric carbon dioxide (CO_2) levels, thereby accelerating global warming (Hansen *et al.*, 2019). Historical temperature data reveal an approximate global increase of 1.1°C since the late 19th century, primarily driven by human-induced greenhouse gas emissions (IPCC, 2021). Climate change has noticeable effects on multiple sectors, including agriculture, water resources, and biodiversity. Shifts in temperature and precipitation patterns are already impacting crop productivity, food security, and water supply (Lobell *et al.*, 2011). Additionally, climate change is increasing the intensity and occurrence of extreme weather events, such as heatwaves, droughts, and floods, which threaten socio-economic stability and livelihoods (Allen *et al.*, 2018).

The primary instruments for modeling the intricate dynamics of the Earth's climate system and forecasting future climatic conditions under diverse scenarios of greenhouse gas emissions are GCMs (IPCC, 2021). New developments in the Coupled Model Intercomparison Project Phase 6 (CMIP6) have improved global simulations of temperature extremes and precipitation patterns by introducing updated Shared Socioeconomic Pathways (SSPs) and refined parameterizations (Eyring *et al.*, 2016; O'Neill *et al.*, 2016). However, their coarse geographical resolution (usually between 100 and 300 km) greatly limits the direct

© GranthaX

use of raw GCM data in localized research. This scale gap fails to capture the microclimatic variability influenced by local topographical features, necessitating the use of statistical or dynamical downscaling techniques to generate localized climate data for precise analytical applications (Maraun *et al.,* 2010; Shaikh *et al.,* 2022).

Moreover, GCM daily weather outputs often show systemic inaccuracies, including overestimation of light precipitation occurrences or distortion of temperature extremes, even after geographic downscaling (Themeßl *et al.,* 2011). Bias correction is a necessary precondition for reliable yield forecasting since process-based agricultural models such as APSIM and CANEGRO are extremely sensitive to daily meteorological inputs (Ruane *et al.,* 2016). As recently shown in South Asian climate assessments, methods like Empirical QM (EQM) are frequently used to match GCM-projected baseline data with observed historical distributions (Cannon *et al.,* 2015; Mishra *et al.,* 2020). Finally, current research strongly supports a multi-model ensemble strategy to reduce the structural uncertainties present in any one climate model. Researchers can more accurately measure climate uncertainty by combining outputs from several CMIP6 GCMs. This gives them a stronger basis on which to assess how future climatic variability may affect sugarcane phenology and regional agricultural systems (Wallach *et al.,* 2018).

Various GCMs based climate change projections studies revealed that the temperature will rising in different climate change scenarios (RCPs and SSPs) due to increasing emission of GHGs (greenhouse gases). Recent studies utilizing bias-corrected climate models project significantly warmer and wetter futures for the Indian subcontinent, raising concerns for agricultural and hydrologic stability. On a broader scale, Mishra et al. (2020) applied CMIP6 models to project a 3–5°C temperature rise and a 13–30% increase in precipitation across South Asia by 2100. These regional trends are supported by localized assessments, such as Shaikh et al. (2022), who modelled the Hathmati River Basin in Western India under the RCP4.5 scenario and projected an ~8.5% increase in both precipitation and temperatures for the 2050s.

The study primarily aimed to project temperature and rainfall trends under two SSPs (shared socioeconomic pathways) scenarios.

2. Datasets

2.1 NASA Global Daily Downscaled Projections (GDDP) CMIP6 dataset

The NASA GDDP-CMIP6 dataset provides high-resolution daily climate projections based on 34 GCMs from the CMIP6. It offers a spatial resolution of 0.25° × 0.25° (~25 km) globally and includes key climate parameters such as daily maximum temperature (Tmax), minimum temperature (Tmin), and daily precipitation. The dataset spans the historical period from 1950 to 2014 and future projections from 2015 to 2100 under different SSPs scenarios, including SSP245 (moderate emissions) and SSP585 (high emissions).

3. Methodology

3.1 Bias correction in GCMs output

GCMs are widely used to simulate climatic variables over the long periods and large spatial scales. However, GCM outputs often exhibit biases due to factors like coarse spatial resolution, simplifications in physical processes, and differences in topographical or regional characteristics. These biases can lead to inaccuracies when using GCM data for regional climate impact assessments, crop modeling, or hydrological studies. Bias correction is essential to adjust GCM outputs, bringing them closer to observed historical data, ensuring more reliable projections for regional applications. The study employed LS and QM as bias correction methods to adjust biases in model-simulated data and ensure alignment with observed historical data.

3.2 GCMs selection strategy

Historical data for Tmax, Tmin, and rainfall were retrieved from 34 CMIP6 GCMs spanning the period 1991–2014. Correction functions were developed for the period 1991–2009 using two bias correction methods: LS and QM. The validation of these correction functions was performed by comparing the model-simulated historical data for 2009–2014 with the corresponding observed data. RMSE and Kling-Gupta Efficiency (KGE) were used as statistical metrics to assess the accuracy of the simulated data. Based on these statistical comparisons, the top four to five GCMs were selected, prioritizing those with the lowest RMSE and highest KGE scores under the both bias correction methods. The entire workflow for climate change projection is illustrated in Figure 1.

4. Results and Discussion

4.1 Bias correction in data

Bias correction is essential for improving the reliability of climate model outputs by aligning them with observed datasets. This process addresses systematic deviations (biases) in GCMs or regional climate models (RCMs), ensuring the simulated data is more realistic for both historical analysis and future projections. Figure 2A, showed the RMSE values without bias correction (blue bars) are significantly higher for all GCMs compared to the values with bias correction methods for Tmax. LS bias correction

© GranthaX

(orange bars) shows moderate improvement by reducing RMSE across most models. However, QM bias correction (green bars) consistently outperforms the LS method, resulting in the lowest RMSE values. This indicates that QM effectively aligns Tmax model outputs closer to observed data by correcting distributional biases.

Similar trends are observed for Tmin. Without bias correction, RMSE values are relatively higher, especially for outlier models like BCC-CSM2-MR, where RMSE spikes abnormally. LS reduces errors, but it is less effective in extreme cases. QM significantly improves the accuracy for most models, as reflected in consistently lower RMSE values. This highlights the importance of addressing distributional mismatches, particularly for Tmin (Figure 2B).

For precipitation (Figure 2C), RMSE values are generally much higher compared to temperature variables, emphasizing the challenge of accurately simulating precipitation patterns in GCMs. Without bias correction, RMSE is excessively high across most models, reflecting substantial deviations from observed data. LS shows limited improvements, suggesting its inability to correct complex biases in precipitation data. QM delivers the best performance, with noticeable reductions in RMSE for almost all models, underscoring its capability to address both mean and variability biases effectively.

The comparison clearly demonstrates the effectiveness of bias correction methods, particularly QM, in reducing errors and improving the reliability of GCM outputs. LS offers a straightforward approach for bias correction but falls short in handling more complex or extreme deviations, especially in precipitation data. Researchers such as Enayati *et al.,* (2021); Guo *et al.,* (2019); Maraun, (2013); Panjwani *et al.,* (2023); Rohith and Cibin, (2024) and Lader *et al.,* (2017) employed QM for bias correction in GCM outputs. Meanwhile, Mahmood *et al.,* (2018) and Mahmood and Jia (2017) utilized the LS method to bias correction in GCM data. These studies highlight the diversity of approaches in refining GCM outputs for improved accuracy.

4.2 Selection of CMIP6 GCMs models

Among the 34 CMIP6 GCMs models, the top four to five models were selected based on their performance. The selection criteria included a low RMSE and a high Kling-Gupta Efficiency (KGE). These selected models are highlighted in green in Table 1. For maximum temperature, the selected models were ACCESS-CM2, CMCC-ESM2, GFDL-CM4, KIOST-ESM, and TaiESM1, which demonstrated low RMSE and high KGE values under QM bias correction method. Notably, ACCESS-CM2 recorded the lowest RMSE (0.14 °C) and the highest KGE (0.85), indicating its excellent agreement with observed data. For minimum temperature, ACCESS-ESM1-5, CNRM-ESM2-1, EC-Earth3, and INM-CM5-0 were identified as the best-performing models under linear scaling. Among these, EC-Earth3 showed the highest KGE (0.63), while CNRM-ESM2-1 achieved the lowest RMSE (0.31°C), highlighting their reliability in capturing temperature minima.

Rahman and Pekkat (2024) identified GCMs ensembles for temperature projections over the Indian subcontinent, with KIOST-ESM, MRI-ESM2-0, MIROC6, NESM3, and CanESM5 for maximum temperature, and E3SM-1-0, NESM3, CanESM5, GFDL-CM4, INM-CM5-0, and CMCC-ESM2 for minimum temperature.

Rainfall simulation posed a greater challenge due to its high spatial and temporal variability. The selected models for rainfall were ACCESS-CM2, KACE-1-0-G, MPI-ESM1-2-LR, MRI-ESM2-0, and TaiESM1. QM significantly improved their performance, with TaiESM1 achieving high KGE values (0.76) and KACE-1-0-G recording the lowest RMSE (312 mm). Across all variables, QM consistently outperformed Linear Scaling, effectively reducing biases, and enhancing the accuracy of GCM outputs. After selecting the optimal GCMs based on their performance metrics, a multi-model ensemble approach was applied to improve the reliability and robustness of climate projections. Sharma and Kale (2022) selected five GCMs models namely NOrESM1-M, bcc-csm1-1, CNRM-CM5, MIROC-ESM, and GFDL-CM3 for projecting the annual rainfall of Surat city.

4.3 Climate Change Projection Under SSPs Scenario

4.3.1 Maximum temperature projection

The projected maximum temperature rise under different climate scenarios (SSP245 and SSP585) is analyzed from 2020 to 2100, as depicted in Figure 3A. The baseline temperature is set at 32.36°C, with deviations plotted for each scenario. The results indicate a consistent upward trend in maximum temperature rise, with significant differences between the two scenarios.

© GranthaX

GranthaX
Independent Scholarly Publishing

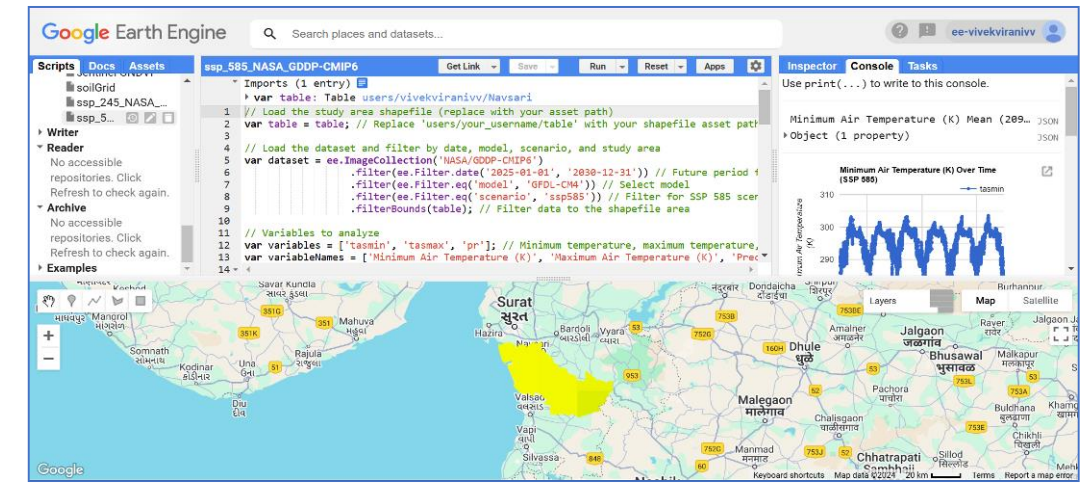

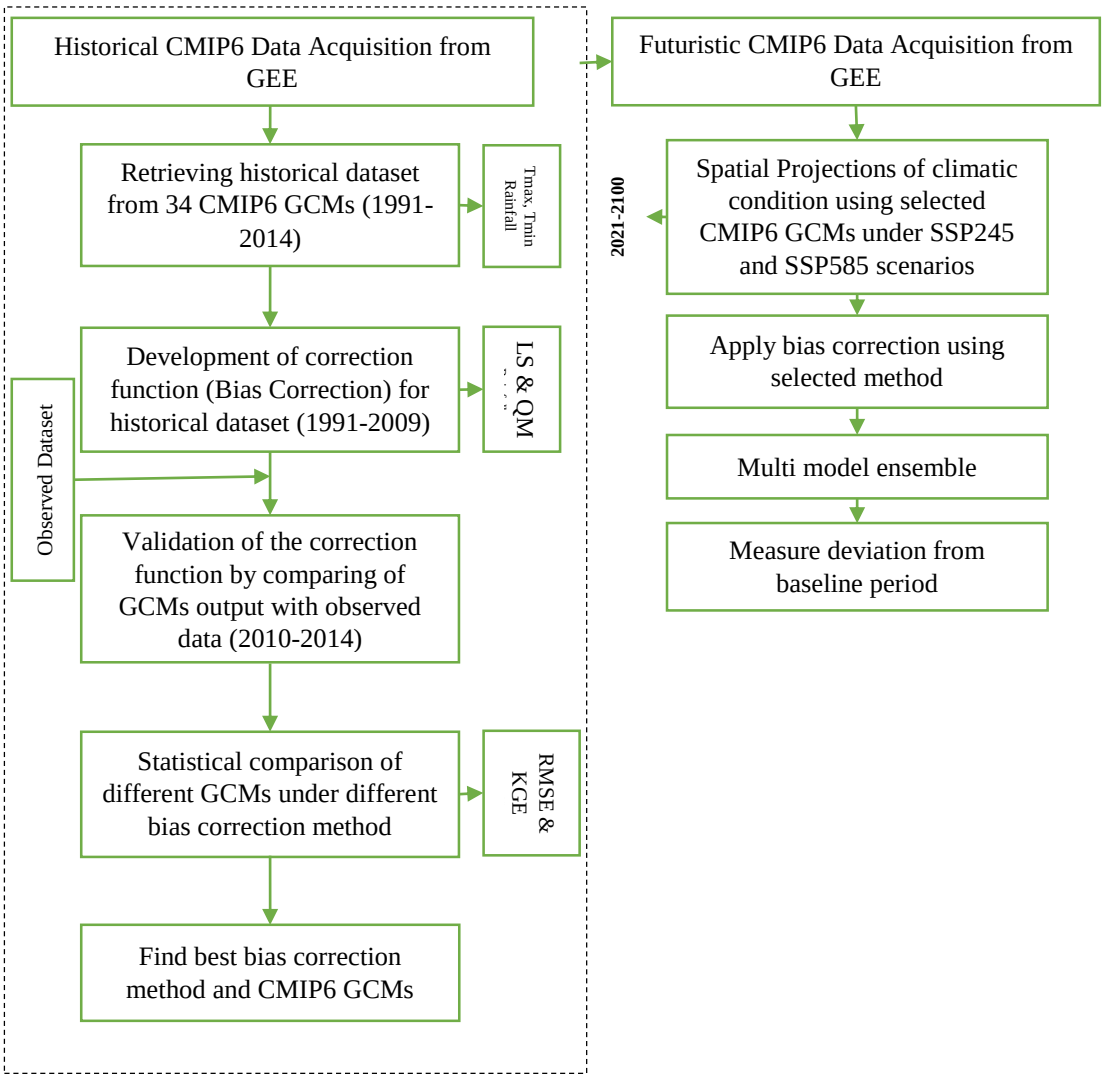

Fig 1. Workflow for bias correction and climatic projections using CMIP6 GCMs and GEE

© GranthaX

GranthaX
Independent Scholarly Publishing

Table 1 Values of performance indicators and selected GCM ensembles for Tmax, Tmin, and rainfall

Sr. No.	GCM model	Maximum Temperature				Minimum Temperature				Rainfall			
		Linear Scaling (LS)		Quantile Mapping (QM)		Linear Scaling (LS)		Quantile Mapping (QM)		Linear Scaling (LS)		Quantile Mapping (QM)	
		RMSE (°C)	KGE	RMSE (°C)	KGE	RMSE (°C)	KGE	RMSE (°C)	KGE	RMSE (°C)	KGE	RMSE (mm)	KGE
1	ACCESS-CM2	0.186	0.67	**0.147**	**0.85**	0.732	-0.41	1.120	-0.41	445	0.43	**416**	**0.47**
2	ACCESS-ESM1-5	0.467	-0.28	0.480	-0.33	**0.483**	**0.38**	0.961	0.05	766	-0.21	757	-0.43
3	BCC-CSM2-MR	0.496	-0.26	0.458	-0.53	0.766	-0.79	0.897	-0.73	520	-0.58	559	-0.41
4	CESM2	×	×	×	×	×	×	×	×	905	-0.27	599	0.05
5	CESM2-WACCM	×	×	×	×	×	×	×	×	825	-0.49	761	-0.52
6	CMCC-CM2-SR5	0.752	-0.39	0.533	0.07	0.662	-0.47	1.282	-1.62	732	-0.22	673	-0.09
7	CMCC-ESM2	0.386	0.59	**0.214**	**0.71**	0.685	-0.83	0.893	-0.80	1038	-0.15	826	-0.83
8	CNRM-CM6-1	0.320	0.55	0.351	0.44	0.474	-0.12	1.011	0.00	546	-0.09	623	0.01
9	CNRM-ESM2-1	0.604	-0.16	0.526	-0.35	**0.310**	**0.43**	0.716	0.55	869	-0.77	959	-0.75
10	CanESM5	0.617	-0.69	0.554	-0.85	0.754	0.69	1.228	0.05	735	-0.56	747	-0.70
11	EC-Earth3	0.698	-0.37	0.508	0.04	**0.501**	**0.63**	0.857	0.61	790	-0.08	731	-0.08
12	EC-Earth3-Veg-LR	0.475	0.38	0.755	-0.46	0.849	-0.86	1.131	-0.99	556	0.05	640	-0.06
13	FGOALS-g3	0.302	0.02	0.313	0.18	0.949	0.08	1.251	0.00	993	-0.62	863	-0.67
14	GFDL-CM4	0.257	0.59	**0.165**	**0.81**	0.722	-0.81	1.166	-0.90	572	0.15	572	0.00
15	GFDL-ESM4	0.624	-0.23	0.450	0.13	0.663	-0.96	1.045	-1.12	605	0.17	462	0.53
16	GISS-E2-1-G	0.216	0.78	0.278	0.40	0.625	-0.36	0.883	-0.51	521	-0.77	589	-0.76
17	HadGEM3-GC31-LL	0.356	0.34	0.314	0.47	1.018	-0.95	1.198	-0.91	931	-0.34	743	-0.04
18	HadGEM3-GC31-MM	0.409	0.01	0.357	-0.09	0.686	-0.54	0.987	-0.81	553	-0.50	566	-0.48
19	IITM-ESM	×	×	×	×	×	×	×	×	863	-0.82	884	-0.75
20	INM-CM4-8	0.411	0.34	0.445	0.00	0.683	-0.25	1.164	-0.09	585	-0.06	695	-0.32
21	INM-CM5-0	0.325	0.00	0.337	-0.48	**0.329**	**0.20**	0.960	0.29	412	0.43	485	0.44
22	IPSL-CM6A-LR	0.592	-0.79	0.583	-0.75	0.758	0.40	1.129	0.04	1195	-1.03	1009	-0.98
23	KACE-1-0-G	0.340	0.20	0.312	0.15	0.615	-0.91	1.095	-0.87	301	0.56	**312**	**0.73**
24	KIOST-ESM	0.488	0.31	**0.306**	**0.70**	0.528	-0.72	1.014	-0.55	508	0.62	492	0.60
25	MIROC-ES2L	0.782	-0.73	0.460	-0.40	0.338	0.22	0.550	0.20	854	-0.89	849	-0.93
26	MIROC6	0.871	-0.78	0.583	-0.47	0.639	-0.59	1.363	-1.76	881	-0.56	719	-0.42
27	MPI-ESM1-2-HR	0.560	0.19	0.384	0.21	0.394	0.04	0.688	0.12	729	0.00	613	0.08
28	MPI-ESM1-2-LR	0.430	0.05	0.331	-0.05	0.449	-0.13	0.811	-0.14	463	0.57	**419**	**0.61**
29	MRI-ESM2-0	0.874	-0.12	1.095	-0.80	0.583	-0.61	1.141	-0.05	750	0.09	**443**	**0.67**
30	NESM3	0.693	0.47	0.511	0.02	0.543	-0.56	1.120	-1.13	362	0.61	331	0.57
31	NorESM2-LM	0.556	-0.30	0.421	-0.17	0.669	-0.79	1.228	-1.29	725	-0.72	725	-0.60
32	NorESM2-MM	0.956	-0.90	0.547	-0.61	0.598	-0.23	0.837	-0.49	1011	-0.59	761	-0.33
33	TaiESM1	0.653	-0.10	**0.163**	**0.67**	1.094	-0.38	1.002	0.00	574	0.54	**421**	**0.76**
34	UKESM1-0-LL	0.520	-0.81	0.486	-0.63	0.496	0.03	0.892	0.04	726	-0.48	648	-0.24

(Highlighted models are selected for climate change projection)

© GranthaX

GranthaX
Independent Scholarly Publishing

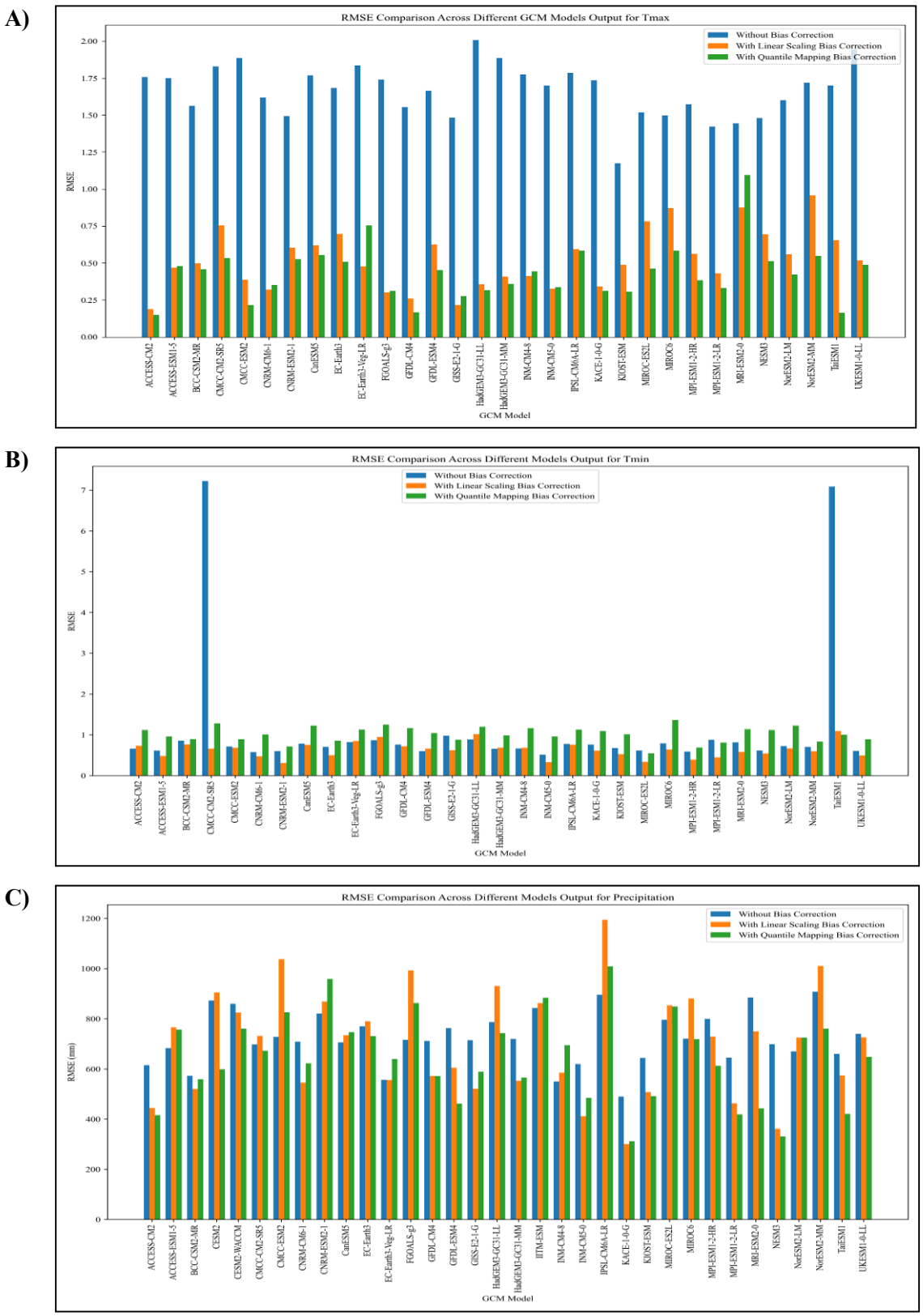

Fig 2. RMSE comparison for **A).** Tmax, **B).** Tmin, and **C).** precipitation across different GCM models under three scenarios

© GranthaX

GranthaX
Independent Scholarly Publishing

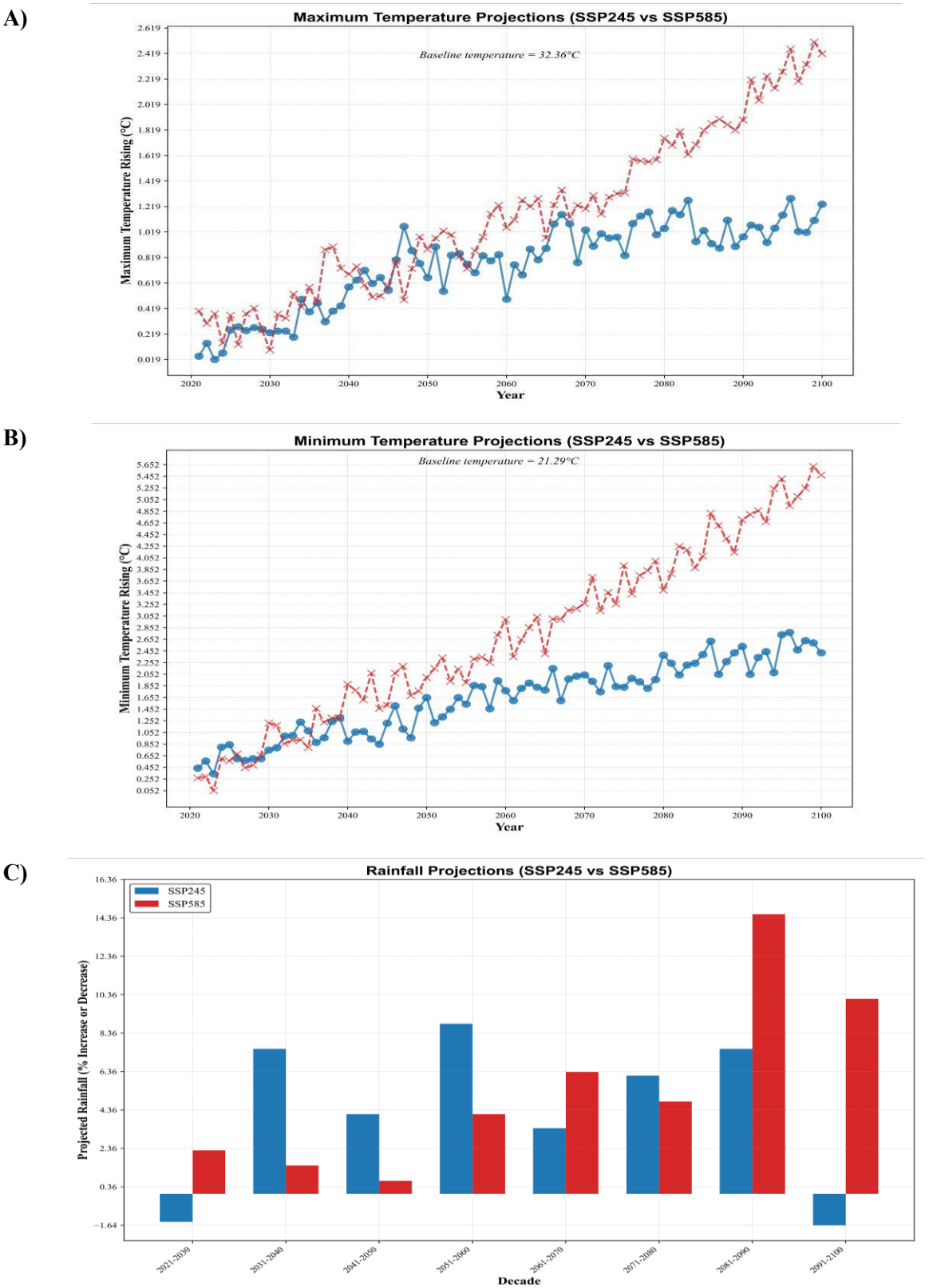

Fig 3. **A).** Maximum temperature, **B).** Minimum temperature, and **C).** Rainfall variation (%) projections under SSP245 and SSP585 scenarios from 2020 to 2100

© GranthaX

GranthaX
Independent Scholarly Publishing

Under the SSP245 scenario, temperature increases are gradual, showing fluctuations but remaining relatively stable after 2070. The variations suggest possible mitigation efforts that limit the extent of temperature rise, although an overall increasing trend is evident. By contrast, the SSP585 scenario, represented by red crosses, exhibits a steeper rise in maximum temperature. The trend suggests that if high greenhouse gas emissions continue, the temperature could rise beyond 2.4°C by the end of the century, which is significantly higher than in SSP245. Mishra *et al.,* (2020) reported that the maximum temperature is projected to rise by 3 to 4°C under the SSP585 scenario by the end of the 21st century across Indian sub-continental river basins.

The widening gap between the two scenarios after 2060 highlights the impact of different emission pathways. While SSP245 shows a moderate increase, the SSP585 trajectory suggests an accelerated warming trend, likely leading to more severe climate-related consequences. These results emphasize the critical need for stringent mitigation measures to limit global warming and its associated risks. The findings align with existing climate models that suggest higher high-emission scenarios, regions could experience intensified rainfall events, potentially leading to flooding and other hydrological extremes. Interestingly, a sharp decrease is projected in the 2091–2100 period, highlighting the unpredictability of precipitation under unchecked emissions. Sharma and Kale (2022) also reported that flood risks are exacerbated by increased precipitation under high-emission scenarios in and around Surat city, a region geographically proximate to present study area. Mishra *et al.,* (2020) also reported a substantial increase in mean annual rainfall, with a median rise of 23% under the SSP585 scenario by the end of 21st century across Indian sub-continental river basins.

When comparing rainfall projections to temperature trends, a key observation is that while temperature consistently rises under both scenarios, rainfall patterns exhibit greater variability. This aligns with climate models suggesting that warming influences precipitation differently across regions, leading to more erratic and extreme weather events. The results emphasize the importance of adaptive water resource management strategies to mitigate the risks of both excessive rainfall and potential droughts in the future. Shaikh *et al.,* (2022) reported a significant increase in precipitation, minimum, and maximum temperatures compared to the baseline over the western India. They concluded that these projected changes could exacerbate water stress and increase the likelihood of severe events, highlighting the need for effective mitigation strategies and management measures to minimize adverse impacts. Pandey (2023) projected that future temperatures will increase across different parts of Gujarat under both RCP 4.5 and RCP 8.5 scenarios, with varying magnitudes. Similarly, rainfall is also expected to increase.

4.3.2 Minimum temperature projection

The projected minimum temperature rise under the SSP245 and SSP585 scenarios from 2020 to 2100 is presented in Figure 3B. The baseline temperature is set at 21.29°C, with variations shown for each scenario. The results indicate a steady increase in minimum temperatures over time, with a significant difference between the two scenarios. Under the SSP245 scenario, minimum temperatures show a gradual upward trend with some fluctuations but remain relatively stable after 2070. This suggests that moderate mitigation efforts could help limit extreme warming, though an overall increase in minimum temperature persists. Conversely, the SSP585 scenario, represented by red crosses, exhibits a more pronounced increase in minimum temperature, surpassing 5.6°C by the end of the century. The accelerated rise under SSP585 suggests that in the absence of aggressive mitigation strategies, nighttime and seasonal minimum temperatures could rise dramatically, impacting ecosystems, agriculture, and human health. Mishra *et al.,* (2020) reported that the minimum temperature is projected to rise by 3 to 5°C under the SSP585 scenario by the end of the 21st century across Indian sub-continental river basins.

When comparing minimum and maximum temperature projections, a few key differences emerge. While both follow an increasing trend, the minimum temperature rise is generally more pronounced than the maximum temperature rise. This result is in good agreement with the findings of Mishra *et al.,* (2020).

4.3.3 Rainfall projection

The projected rainfall variations under SSP245 and SSP585 scenarios from 2021 to 2100 are illustrated in Figure 3C. The graph presents decadal changes in rainfall, expressed as a percentage increase or decrease relative to baseline levels. The results indicate fluctuations in precipitation patterns, with differences between the two climate scenarios becoming more pronounced in the later decades.

Under the SSP245 scenario, rainfall changes remain relatively moderate, with both increases and decreases observed across different decades. Early projections (2021–2040) show modest changes, while a more consistent increasing trend emerges after 2050. However, the fluctuations suggest that while moderate mitigation efforts could help stabilize rainfall variations, uncertainties in precipitation trends remain. In contrast, the SSP585 scenario exhibits more extreme variations. While initial decades show moderate increases, rainfall projections

© GranthaX

become significantly higher in later years (increase up to 14.50%), particularly in the 2081–2090 decade, where precipitation surges dramatically. This suggests that under high-emission scenarios, regions could experience intensified rainfall events, potentially leading to flooding and other hydrological extremes. Interestingly, a sharp decrease is projected in the 2091–2100 period, highlighting the unpredictability of precipitation under unchecked emissions. Sharma and Kale (2022) also reported that flood risks are exacerbated by increased precipitation under high-emission scenarios in and around Surat city, a region geographically proximate to present study area. Mishra *et al.,* (2020) also reported a substantial increase in mean annual rainfall, with a median rise of 23% under the SSP585 scenario by the end of 21st century across Indian sub-continental river basins.

When comparing rainfall projections to temperature trends, a key observation is that while temperature consistently rises under both scenarios, rainfall patterns exhibit greater variability. This aligns with climate models suggesting that warming influences precipitation differently across regions, leading to more erratic and extreme weather events. The results emphasize the importance of adaptive water resource management strategies to mitigate the risks of both excessive rainfall and potential droughts in the future. Shaikh *et al.,* (2022) reported a significant increase in precipitation, minimum, and maximum temperatures compared to the baseline over the western India. They concluded that these projected changes could exacerbate water stress and increase the likelihood of severe events, highlighting the need for effective mitigation strategies and management measures to minimize adverse impacts. Pandey (2023) projected that future temperatures will increase across different parts of Gujarat under both RCP 4.5 and RCP 8.5 scenarios, with varying magnitudes. Similarly, rainfall is also expected to increase.

5. Conclusion

This study provides a comprehensive assessment of the projections of climate change in South Gujarat under the SSP245 and SSP585 scenarios. The findings reveal that rising temperatures and shifting rainfall patterns could significantly influence sugarcane yield, underscoring the vulnerability of the crop to future climate change. Climate models, carefully selected based on their ability to replicate regional climate patterns, offer critical insights for projecting future conditions and informing adaptation strategies.

Our results highlight the necessity of integrating climate-resilient agricultural practices to mitigate the adverse effects of climate change. Furthermore, this study emphasizes the crucial role of bias correction in enhancing the reliability of climate projections, ensuring more accurate impact assessments. By combining robust climate modeling with advanced crop simulation techniques, we contribute to a deeper understanding of climate risks in crops production. Moving forward, developing region-specific adaptation strategies, and leveraging advanced crop simulation models will be essential for sustaining crop productivity in a changing climate, ultimately supporting food security and agricultural sustainability in South Gujarat and beyond.

Acknowledgments

We extend our gratitude to colleagues and researchers whose valuable insights contributed to this study. We acknowledge the availability of climate data from Data Source, e.g., CMIP6, IMD, NASA, as well as the NAU. Lastly, we express our appreciation to our families and peers for their encouragement throughout this research.

Declarations

Author contributions

V. B. Virani: Conceptualization, Methodology, Data Collection, Processing, and Analysis. **Dr. M. H. Amlani:** Writing - Original Draft, Visualization. **B. M. Mote**: Writing - Original Draft.

Funding Statement

This research was conducted without external financial support, reflecting the independent efforts and commitment of the authors.

Data Availability

The datasets generated and/or analysed during the current study are available in a publicly accessible repository.

Competing Interests

The authors have no relevant financial or non-financial interests to disclose.

References

Allen, M.R., Dube, O.P., Solecki, W., Aragón-Durand, F., Cramer, W., Humphreys, S., & Zickfeld, K. (2018). Framing and context. *Global Warming of 1.5°C: An IPCC Special Report on the Impacts of Global Warming of 1.5°C Above Pre-Industrial Levels*.

Cannon, A.J., Sobie, S.R., & Murdock, T.Q. (2015). Bias correction of GCM precipitation by quantile mapping: How well do methods preserve changes in quantiles and extremes? *Journal of Climate*, 28(17), 6938–6959.

Enayati, M., Bozorg-Haddad, O., Bazrafshan, J., Hejabi, S., & Chu, X. (2021). Bias correction capabilities of

© GranthaX

quantile mapping methods for rainfall and temperature variables. *Journal of Water and Climate Change*, 12(2), 401–419.

Eyring, V., Bony, S., Meehl, G.A., Senior, C.A., Stevens, B., Stouffer, R.J., & Taylor, K.E. (2016). Overview of the Coupled Model Intercomparison Project Phase 6 (CMIP6) experimental design and organization. *Geoscientific Model Development*, 9(5), 1937–1958.

Guo, Q., Chen, J., Zhang, X., Shen, M., Chen, H., & Guo, S. (2019). A new two-stage multivariate quantile mapping method for bias correcting climate model outputs. *Climate Dynamics*, 53, 3603–3623.

Hansen, J., Sato, M., & Ruedy, R. (2019). Global temperature in 2018 and beyond. *Climatic Change*, 154(3–4), 219–232.

Intergovernmental Panel on Climate Change (IPCC). (2021). *Climate Change 2021: The Physical Science Basis.* Cambridge University Press.

IPCC. (2021). *Climate Change 2021: The Physical Science Basis. Contribution of Working Group I to the Sixth Assessment Report of the Intergovernmental Panel on Climate Change*. Cambridge University Press.

Lader, R., Walsh, J.E., Bhatt, U.S., & Bieniek, P.A. (2017). Projections of twenty-first-century climate extremes for Alaska via dynamical downscaling and quantile mapping. *Journal of Applied Meteorology and Climatology*, 56(9), 2393–2409.

Lobell, D.B., Schlenker, W., & Costa-Roberts, J. (2011). Climate trends and global crop production since 1980. *Science*, 333(6042), 616–620.

Mahmood, R., & Jia, S. (2017). An extended linear scaling method for downscaling temperature and its implication in the Jhelum River basin, Pakistan, and India, using CMIP5 GCMs. *Theoretical and Applied Climatology*, 130, 725–734.

Mahmood, R., Jia, S., Tripathi, N.K., & Shrestha, S. (2018). Precipitation extended linear scaling method for correcting GCM precipitation and its evaluation and implication in the transboundary Jhelum River basin. *Atmosphere*, 9(5), 160.

Maraun, D. (2013). Bias correction, quantile mapping, and downscaling: Revisiting the inflation issue. *Journal of Climate*, 26(6), 2137–2143.

Maraun, D., Wetterhall, F., Ireson, A.M., et al. (2010). Precipitation downscaling under climate change: Recent developments to bridge the gap between dynamical models and the end user. *Reviews of Geophysics*, 48(3).

Mishra, V., Bhatia, U., & Tiwari, A.D. (2020). Bias-corrected climate projections for South Asia from Coupled Model Intercomparison Project-6. *Scientific Data*, 7(1), 1–13.

O'Neill, B.C., Tebaldi, C., van Vuuren, D.P., et al. (2016). The Scenario Model Intercomparison Project (ScenarioMIP) for CMIP6. *Geoscientific Model Development*, 9(9), 3461–3482.

Pandey, V. (2023). Climate variability, trends, projections and their impact on different crops: A case study of Gujarat, India. *Journal of Agrometeorology*, 25(2), 224–238.

Panjwani, S., Naresh Kumar, S., & Ahuja, L. (2021). Bias correction of GCM data using quantile mapping technique. *Proceedings of the International Conference on Communication and Computational Technologies (ICCCT-2019)*, 617–621.

Rahman, A., & Pekkat, S. (2024). Identifying and ranking of CMIP6-global climate models for projected changes in temperature over Indian subcontinent. *Scientific Reports*, 14(1), 3076.

Rohith, A.N., & Cibin, R. (2024). An extremes-weighted empirical quantile mapping for global climate model data bias correction for improved emphasis on extremes. *Theoretical and Applied Climatology*, 1–9.

Ruane, A.C., Hudson, N.I., Asseng, S., et al. (2016). Multi-wheat-model ensemble responses to interannual climate variability. *Environmental Modelling & Software*, 81, 86–101.

Shaikh, M.M., Lodha, P., Lalwani, P., & Mehta, D. (2022). Climatic projections of Western India using global and regional climate models. *Water Practice and Technology*, 17(9), 1818–1825.

Sharma, A., & Kale, G.D. (2022). Ranking of general circulation models for Surat City by using a hybrid approach. *Water Practice and Technology*, 17(10), 2186–2198.

Themeßl, M.J., Gobiet, A., & Leuprecht, A. (2011). Empirical-statistical downscaling and error correction of daily precipitation from regional climate models. *International Journal of Climatology*, 31(10), 1530–1544.

Wallach, D., Martre, P., Liu, B., et al. (2018). Multimodel ensembles improve predictions of crop-environment-management interactions. *Global Change Biology*, 24(11), 5072–5083.

Publisher's Note: GranthaX remains neutral with regard to jurisdictional claims in published maps and institutional affiliations.

© GranthaX